Arabian Journal for Science and Engineering (2023) 48:47–61
https://doi.org/10.1007/s13369-022-06796-4

RESEARCH ARTICLE-BIOLOGICAL SCIENCES

Surface Functionalization of Graphene Oxide with Silver Nanoparticles Using Phyto Extract and its Antimicrobial Properties Against Biological Contaminants

Abhaysinh Salunkhe[1] · Shalini Tandon[1] · Swapnil Dudhwadkar[1]

Received: 16 June 2021 / Accepted: 6 March 2022 / Published online: 30 June 2022

Abstract
Enhancing stability and antimicrobial properties of nanomaterial and its application in biological field is a burgeoning field of research. In this study, silver nanoparticle decorated graphene oxide (Ag^0NP@GO) nanocomposite were synthesized using ecofriendly method. *Lantana camara* plant extract was selected as a green reducing agent. High phytochemical constituents [Total Phenols—10.44 (TAE) and 9.95 (GAE), Total Tannins—5.98 (TAE) and 5.75 (GAE), Total Flavonoids—8687 mg QE/Kg] in aqueous phytoextract was responsible for the reduction of Ag^+ into silver nanoparticles (Ag^0NP). The successful formation of nanocomposite was confirmed by the characterization of GO and Ag^0NP@GO by UV–VIS, FTIR spectroscopy and XRD. Morphology and size of nanocomposite was confirmed with SEM–EDX and HR-TEM imaging. Results showed that silver nanoparticles (Ag^0NPs) with an average size of 51 and 76 nm from Debye-Shrerrer's equation and SEM, respectively were impregnated onto GO sheets. The antibacterial activity of synthesized nanocomposite was tested against bacteria and fungus using Kirby-Bauer test. The zone of inhibition was observed for *Bacillus subtilis* (21 mm), *Staphylococcus aureus* (18 mm), *Escherichia coli* (21 mm), *Pseudomonas putida* (21 mm) and *Candida albicans* (31 mm). Complete inhibition of *Aspergillus niger* was found at 400 mg/L. All results of the present study affirmed the potential applications of Ag^0NP@GO as an antimicrobial agent against biological contaminants.

Keywords Graphene oxide · Silver nanoparticle · Antimicrobial · Antifungal · *Lantana camara*

1 Introduction

Silver has inherent antimicrobial properties against various bacteria and is classified under the broad spectrum category [13]. It exhibits wide range of antimicrobial action like interacting with thiol groups in bacterial enzymes and proteins, inhibiting cell division, damaging the cell envelope [6] and interacting with nucleic acid especially altering DNA bases and phosphate groups [65]. Due to less surface area and higher cost, it is difficult to realize the desired concentration of bulk metallic silver materials. Zero valent silver nanoparticles (Ag^0NPs) have larger surface area, which shows effective antimicrobial and anticancer properties with minimal concentration [2, 51]. However, the practical application of silver nanoparticles is often hampered by the self-aggregation or precipitation resulting in loss of antibacterial activity [39]. Therefore, it becomes essential to develop highly stable and dispersed Ag^0NPs. Pristine Ag^0NPs are very difficult to handle in liquid phase also their recovery for reuse, similarly separation of Ag^0NPs in the form of powder is very time consuming and an expensive technique. Hence, attempts have been made by many researchers to couple Ag^0NPs with the other nanostructures in order to overcome the above practical difficulties. Research has been carried out with respect to coating of Ag^0NPs on cotton cellulose [21] or in-situ reduction of Ag^+ ions to Ag^0 NPs on the surface of other nanostructured materials such as nanosilica, nanoclay, or zeolite [8, 10, 38]. Similarly, Ag^0NPs has been successfully used in combination with nanostructured carbon family members such as CNT or multi-walled CNT (MWCNT) [35, 67] activated carbon fibers [66] and newest one is Graphene family members such as Graphene Oxide

✉ Shalini Tandon
tandon.shalini@gmail.com

[1] CSIR-National Environmental Engineering Research Institute, Mumbai Zonal Centre, 89/B, Dr. A.B. Road, Worli, Mumbai, Maharashtra 400018, India

(GO) [44, 68], Reduced Graphene Oxide (RGO) or pristine graphene layers.

In the recent times Graphene oxide (GO) has attracted attention due to its 2D honeycomb lattice structure of carbon atoms [3]. Graphene oxide has high surface area and has carboxylic, carbonyl, hydroxyl and epoxide groups on the sides, thus it is strongly hydrophilic and forms stable colloidal dispersions in water [53]. Silver nanoparticles embedded on graphene oxide (GO- Ag^0NPs) were studied for applications like visible photocatalysis degradation and adsorbent of various dyes like Rhodamine and Indigoamine [47, 70]. The application also include electrochemical sensor for detection of amino acids [42], desalination [61], filtration [34] and heavy metal removal [43]. For the synthesis of GO- Ag^0NPs, a strong chemical reducing agent such as sodium borohydrate, hydrazine monohydrate or polyethylene amine has been used. [7, 15]. The major drawback of these chemical reducing agent is that, they are inflammable, carcinogenic and have cytotoxic properties. However, green chemistry synthesis approach such as natural plants phytoextract based nanoparticle synthesis is a better option. The reactions are completed in a few minutes to few hours at room temperature. Apart from synthesis time, low energy consumption, low cost, less chances of failure and ease of characterization [1] has attracted more attention in recent years.

The aim of the study was to synthesize and characterize silver nanoparticles embedded on the surface of functionalized graphene oxide. The reduction of silver nanoparticles was carried out using *Lantana camara* aqueous leaf extract. *L. camara* (Family—verbenaceae) is also known as wild or red sage. It is considered a waste biomass, notorious weed, which grows profusely and is available worldwide. Scratching, stomachache, rheumatism, wound healing, biliary fever, toothache, bronchitis , antiseptic, and other illnesses have all been treated using different portions of the *L. camara* [16, 25]. Proteins, carbohydrates, common secondary metabolites, and minor components of phytosterols, saponins, tannins, and phycobatannin were found in quantitative phytochemical analyses of *L. camara*. Also, threefold total sugars and maximum amounts of phospholipid content were found in the leaves of *L. camara* [23]. Hence, the presence of phenolics, flavonoids, terpenoids, alkaloids, lipids, proteins, and carbohydrates was attributed for the reduction of Ag^+ to Ag^0 nanoparticles [37]. As a result, this plant extract serves as both a reducing and a capping agent simultaneously, without the use of chemicals. Further, the study also focuses on characterization and testing of these nanocomposites against biological contaminants and arriving at an optimum concentration needed for their inhibition.

2 Material and Methods

2.1 Chemicals, Reagents and Media

Chemicals were purchased locally. Analytical-grade $AgNO_3$, liquor ammonia, $KMnO_4$, H_2O_2 (30%), H_2SO_4 (98%), H_3PO_4 (85%) used in this study were purchased from Merck, India. Graphite flakes were purchased from S. D Fine Chemicals, India. Luria Bertani agar, Mueller Hinton broth and Potato Dextrose agar were purchased from Himedia Ltd, India. Bacterial and Fungal cultures were purchased from National Centre for Cell Science, India.

2.2 Preparation of Aqueous Phyto Extract

For the preparation of aqueous extract, plant material (*Lantana camara*) weighing 2 g was added to 25 mL sterile deionised (DI) water. The mixture was kept overnight in a dark place and gently heated in a microwave oven at 900 Hz for 2–3 min. The extract was then filtered through syringe filtration (porosity 0.45μ) and was preserved in a refrigerator at 4 °C for further use.

2.3 Phyto-Chemical Assay of Prepared Phyto Extract

Total phenol Content (TPC) and Total Tannin content (TTC) were analyzed using Folin-Ciocalteu method [5, 18]. For Total Flavonoids determination, aluminum chloride colorimetric method was used [40]. Plant extract (0.5 mL) was mixed with 1.5 mL of methanol, 0.1 mL of 10% aluminum chloride, 0.1 mL of 1 M potassium acetate and 2.8 mL of deionised water. The reaction mixture was allowed to stand at room temperature for 30 min and the absorbance of the reaction mixture was measured at 415 nm. The calibration curve was prepared by using Quercetin at concentrations of 12.5–100 mg/L in methanol. The reducing power of water extracts of plant material was determined by the method of Oyaizu [31]. For antioxidant assay, DPPH (2, 2-diphenyl-1-picryl-hydrazyl-hydrate) scavenging method was used; 0.1 mL of extracts was mixed with 2.9 mL of 0.1 mM DPPH solution. Negative control was prepared by mixing 0.1 mL of methanol with 2.9 mL of DPPH solution. The radical scavenging activity was calculated in terms of Ascorbic Acid Equivalent [40].

2.4 Synthesis of Graphene Oxide (GO) Nanosheets

Improved Hummer's Method with minor modification was used to make GO nanosheets from natural graphite powder [29, 60]. In a nutshell, graphite powder was added to a low-temperature combination of conc. H_2SO_4 and H_3PO_4 (1:9). Followed by addition of $KMnO_4$ in same reaction vessel and was kept under stirring condition for 12 h at 45 °C. GO

dispersion was obtained by addition of 20 mL 30% H_2O_2. Purification was done by multiple washing with HCl and Type I deionised water until the pH was reached to 7. Finally, the GO nanosheets dispersion were dried at 55 °C overnight.

2.4.1 Phyto-Synthesis of Silver Nanoparticles Embedded Graphene Oxide Nanosheet (Ag^0NP@GO Nanocomposite)

100 mL of GO dispersion (1.005 mg/mL) was added with calculated weight of $AgNO_3$ so that final concentration of Ag^+ ions was 10 mM. This mixture was allowed to stand overnight. Finally, 15 mL of fresh aqueous plant extract of *Lantana camara* was added and mixed vigorously. The above mixture was heated in microwave oven at 900 Hz for 120 s. Dark brown mass was separated by centrifugation at 5000 rpm; pellet was washed thrice with acetone and deionized water followed by drying at 40°C [11]. Dried material was ground and stored for further characterization and antimicrobial studies. During the above synthesis, one set of a blank system (i.e. GO dispersion with 10 mM $AgNO_3$ solution without plant extract) was run parallel to check the effect of microwave on the formation of nanoparticles.

2.5 Characterization of Synthesized Nanocomposite

Characterization of GO, Ag^0NP's and Ag^0NP@GO was done with UV–Visible spectrophotometer (Labtronics, India Model-LT290 with spectral scanning software MetaSpec Pro Ver. 2.0), FT-IR spectra (Bruker, Germany. Model: Vertex 80) by KBr powder pressed pellets method. Energy-dispersive x-ray (EDX) spectrometry and Scanning Electron Microscopy (SEM–EDX, Quanta 2000), HRT- TEM (JEOL, Model: JEM 2100F) and XRD (PANalytical, X' Pert Pro) for confirming the crystal phase formation size of metal nanoparticles based on Debye-Shrerrer's formula.

$$dp = \frac{\mathbf{k}\lambda}{\beta \mathbf{Cos}\theta}$$

where, dp = Average crystallite size (nm), k = Scherrer constant. K = 0.94 for spherical crystallites with cubic symmetry, λ = X-ray wavelength, For XRD, Cu Kα average = 1.54178 A^0, β = FWHM (Full Width at Half Maximum) of, XRD peak, θ = XRD peak position, half of the Bragg angle 2θ (in radians)

2.6 Inhibition of Bacteria using Synthesized Nanocomposite

This test was performed using Agar well diffusion technique [46]. Four bacterial strain (*Escherichia coli, Pseudomonas putida, Bacillus subtilis and Staphylococcus aureus*) were mixed individually in phosphate buffer (pH 7.2), vortexed and optical density adjusted to 0.5 [48]. 1 mL of each bacterial culture was bulk seeded in sterile Luria Bertani molten agar, poured and allowed to solidify. Further, using a sterilized cork borer, wells were dug and 100 μL of synthesized nanocomposite (25, 50, 100, 200, 300, 400 and 500 mg/L) and saline (Control) were added to these wells. The plates were incubated at 37 °C for 24 h. Zone of inhibition were measured and mean values are reported.

2.7 Determination of Minimum Inhibitory Concentration (MIC) and Minimum Bactericidal Concentration (MBC)

MBC is the lowest concentration of antimicrobial that will prevent the growth of an organism, while MIC is the lowest concentration of nanoparticles that will impede the visible growth of a bacterium. In brief, 96 well micro titer plate-based method was adapted, each well was first added with sterile 100 μL the Mueller Hinton broth followed by the 100 μL of varying concentration of nanomaterial in dispersion form. Lastly 50μL bacterial culture of known cell density (O.D at 600 nm adjusted at 0.1) was added. The plates were incubated for 24 h at 37 °C. Inoculating culture in growth media without test samples served as a negative control. Finally, 40μL of INT (p-iodonitrotetrazolium salt) dye solution was added and incubated at 30 °C for 30 min and the color change of dye from yellow to pink by viable bacteria was observed and reported. Bactericidal Concentration (MBC) was evaluated by streaking a loop full of the sample from the wells with concentrations corresponding to MIC and above on sterile nutrient agar plates.

2.8 Antifungal Activity of Synthesized Nanocomposite

Two fungi were used namely, *Candida albicans* and *Aspergillus niger.* For antifungal activity against *Candida,* agar well diffusion technique was used and for *Aspergillus,* disc diffusion method was performed. In brief, sterile potato dextrose agar plates were coated with synthesized nanocomposite using a sterilized glass spreader. Further, sterile paper discs were loaded with fungal spores and were placed at the center of the plate containing nanocomposite. The plates were incubated at 30 °C for 3 to 4 days. The growth of fungus in form of mycelium was compared with that of blank (without nanocomposite).

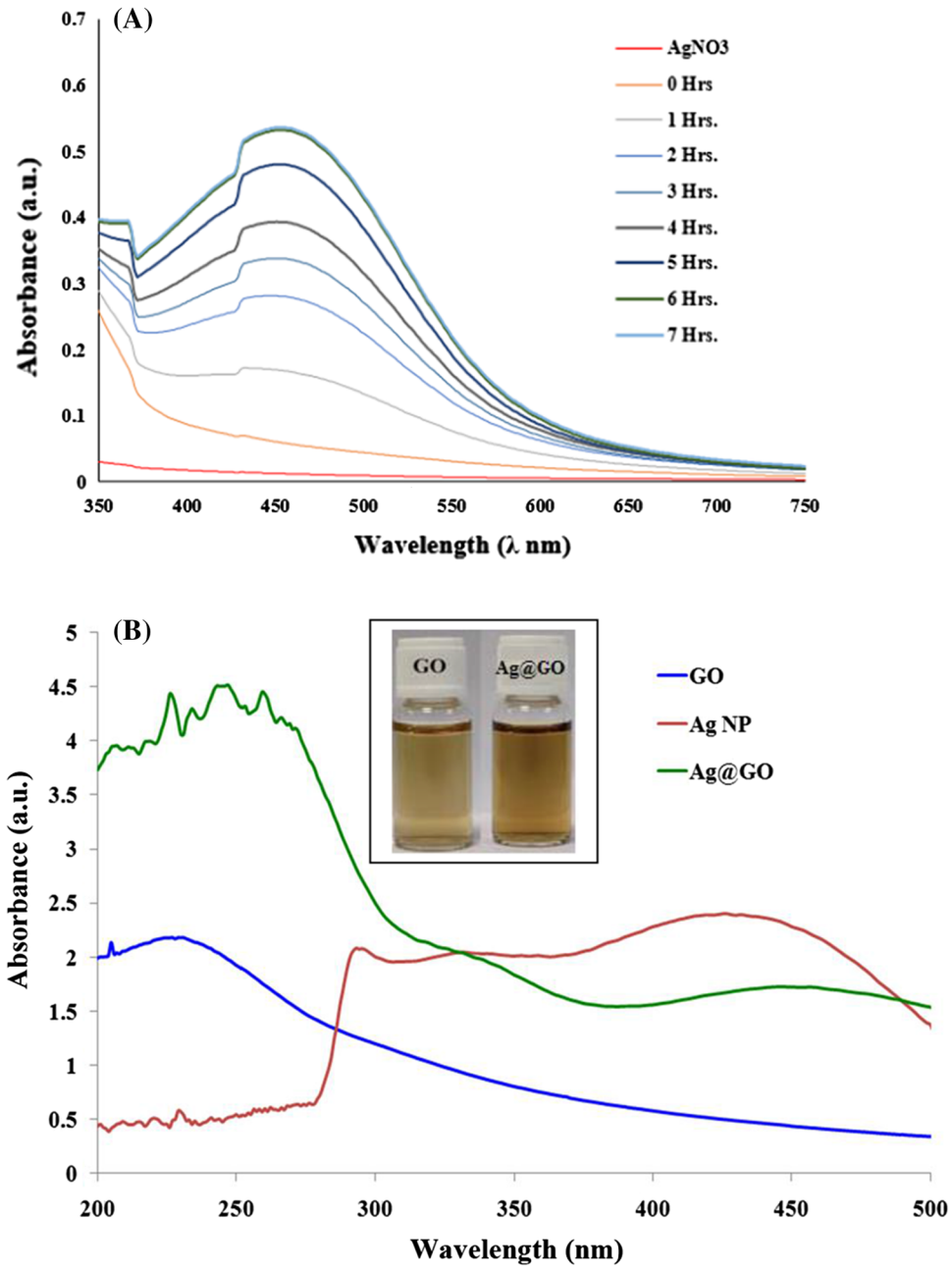

Fig. 1 **A** UV–Vis spectrum of Ag^0NPs synthesized with *Lantana camara* at different reaction time **B** Comparative UV–Visible Spectrum of GO, Ag^0 NPs, and Ag^0NP@GO using *Lantana Camara* plant extract as reducing agent

3 Result and Discussion

3.1 Phyto-Chemical Assay of Prepared Plant Extract

Total Phenolic Content (TPC) was found to be 10.44 (TAE i.e. Tannic Acid Equivalent) and 9.95 (GAE i.e. Gallic Acid Equivalent), respectively. Similarly, Total Tannin Content (TTC) was 5.98 (TAE) and 5.75 (GAE). It was also found that non tannin group of phenolic compounds were also present in significant concentration [4.46 (TAE) and 4.20 (GAE)]. According to DPPH test, 23% Scavenging Activity was observed whereas, Total Flavonoid Content (TFC) was figured as 8687 mg QE/Kg i.e. mg of quercetin equivalent per kg of dry matter. Along with this positive test of Ferric Reducing Antioxidant Power Assay (FRAP) also proved the reduction potential of the phytochemical present in the plant extract. According to a study by Jain et al. [33], nearly 14 compounds were detected and quantified from *Lantana camara* leaves extract by HPLC, namely protocatechuic acid, p-hydroxybenzoic acid, vanillic acid, syringic acid, Vanillin, p-coumaric acid, caffeic acid, gentisic acid, m -coumaric acid, o -coumaric acid, ferulic acid, salicylic acid, t-cinnamic acid and methyl coumarin which were major contributory members in total phenol content of the plant extract.

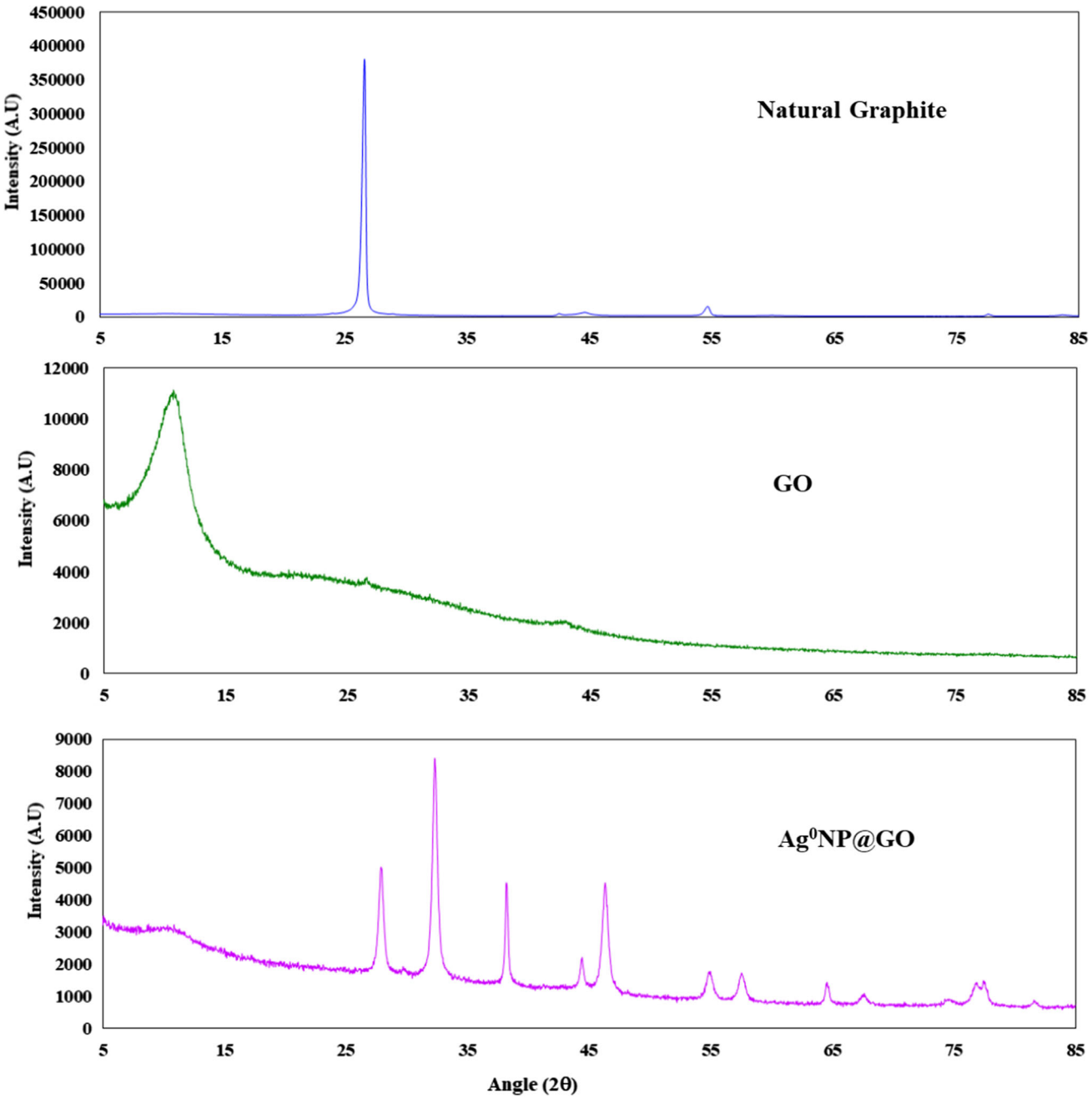

Fig. 2 XRD pattern of Natural Graphite, GO and Ag^0NP@GO synthesized using plant extract as a reducing agent

From overall phytochemical analysis, it was established that the plant extract has enough concentration of Total Phenolic (TPC), tannin (TTC), Flavonoids (TFC) and Antioxidant group of compounds which can act as a potent green reducing agent for the reduction of the metal ions to metal nanoparticles as compared to blank solution. No color change was observed in the blank experiment without the plant extract, thus showing the necessity of the extract for the Ag^+ ions reduction under the experimental conditions. Also, phytoextract act as a stabilizing agent which prevents nanoparticles from the process of agglomeration.

3.2 Synthesis and Characterization of Nanocomposite

When *Lantana camara* plant extract was mixed with freshly prepared silver nitrate solution, the mixture turned from colorless to yellowish brown. The effect of time on biogenic

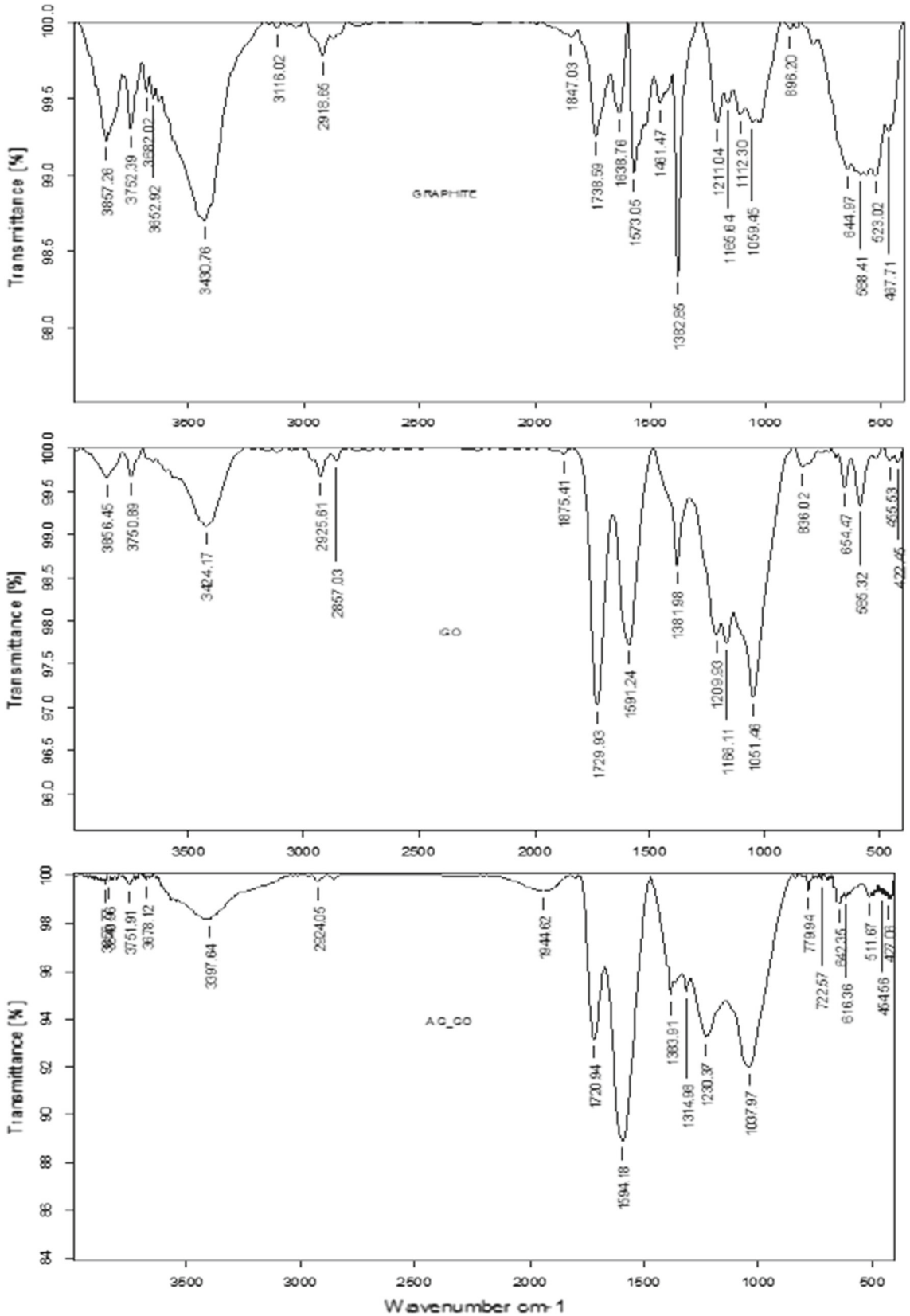

Fig. 3 FTIR Spectrum of Natural Graphite, Graphene Oxide (GO) and Ag^0NP@GO

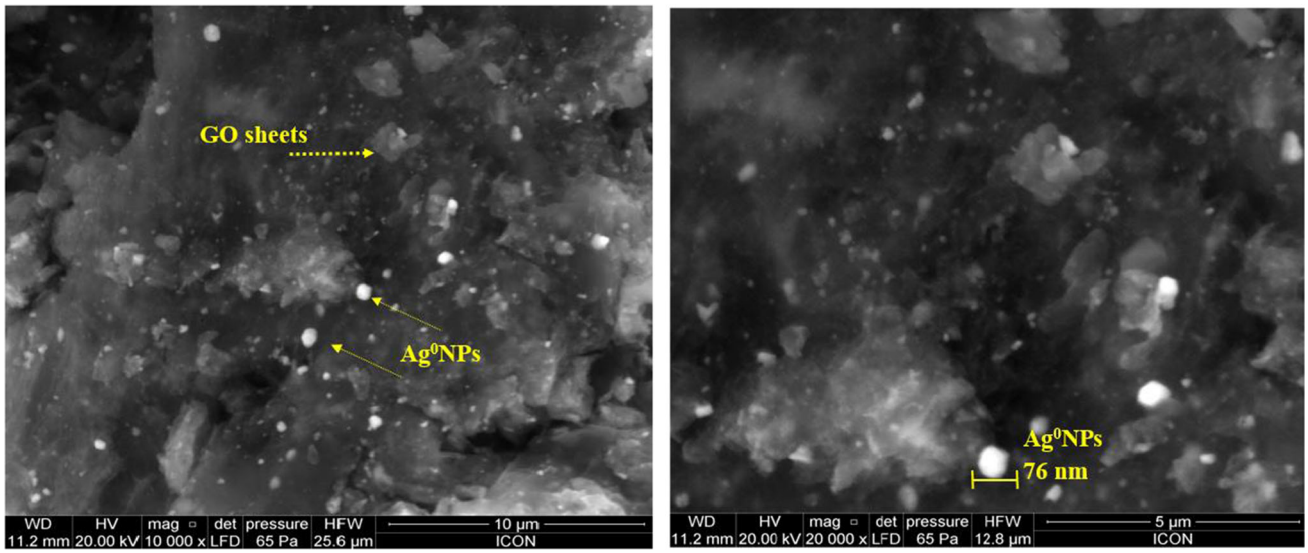

Fig. 4 SEM images of Ag^0NP@GO nanocomposite showing Ag^0NP impregnated in GO nanosheet at the magnification of 10,000X and 20,000X

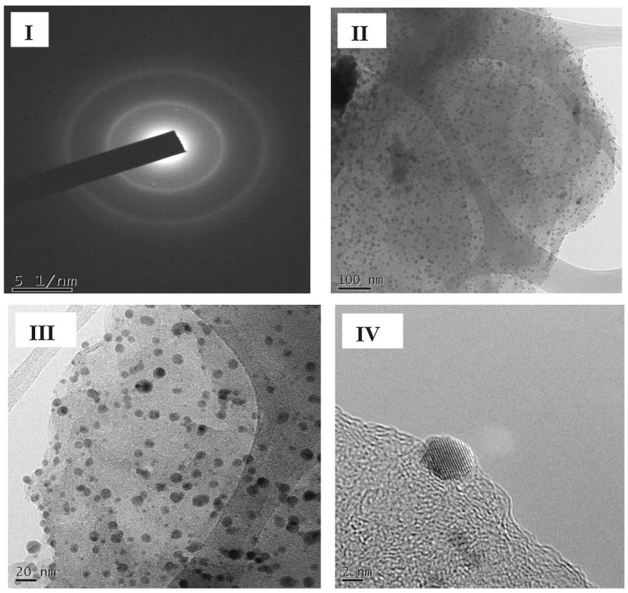

Fig. 5 HR-TEM micrographs of Ag^0NP@GO nanocomposite showing Ag^0 NP impregnated on GO nanosheet (II, III and IV- size distribution of Ag^0NPs anchored to GO sheets and I-selected area electron diffraction (SAED) pattern)

Table 1 Percent weight contribution of elements Ag, C and O atoms in Ag^0NP@GO nanocomposite

Element	Weight%	Atomic%	Net Int	Error %	K ratio
C	22	49	231	5.9	0.2
O	22	37	76	13	0
Ag	56.2	14	895.8	3	0.5

synthesis of Ag^0NPs using *Lantana camara* plant extract is shown in Fig. 1A. A characteristic surface plasmon resonance (SPR) peak observed in the visible region ranging from 400 to 500 nm with λ_{max} of 454 nm was indicative of formation of Ag^0NPs and such peak was not present in the UV–Visible spectra of silver nitrate solution. The peak's intensity grew for the first 6 h and then remained constant. Broadened SPR peak indicated the formation of varied sized poly disperse Ag^0NPs [32]. Position of the SPR peak generally depends upon the shape and size of nanoparticles [20]. Blue or red-shifts in the λ_{max} of the SPR peaks could be related to obtaining Ag^0NPs of various shapes and sizes [49].

Further, UV–Visible spectra of GO, pristine Ag^0NP, and Ag^0NP@GO (Fig. 1B) showed that GO sample had a strong absorption peak at 230 nm, which is due to the π-π^* transitions of aromatic C–C bonds present in GO 2D structure. However, Ag^0NP@GO spectrum showed two different peaks at 240 nm and 445 nm each formed corresponding to the excitation of the plasmon graphitic structure and features of Ag^0NPs, respectively. The near conjugation of Ag^0NP and the GO sheet caused electron transfer and a rise in the transition energy, which caused the red-shift. These findings corroborate the Ag^0NP@GO composite's effective creation. Similar observation was reported by Chen et.al [8] and Chook et.al [12].

XRD was used to examine the crystalline structures of natural graphite and synthesized Graphene oxide. The stacking order of natural graphite and Graphene oxide is connected to the feature diffraction peak. As shown in Fig. 2, natural graphite powder shows an intense peak at 26.6°, whereas the feature diffraction peak of synthesized GO appears at $2\theta = 10.0°$. Natural graphite has an interlayer distance of 3.34 A°, which was raised to 8.833 A° for GO. The presence

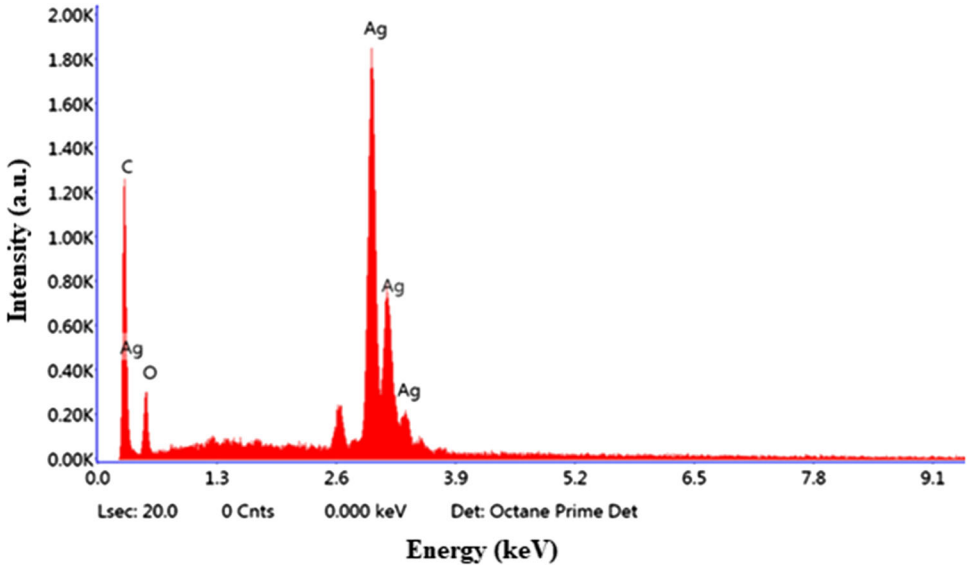

Fig. 6 EDX spectrum showing Elemental composition of the Ag^0NP@GO nanocomposite with peak position

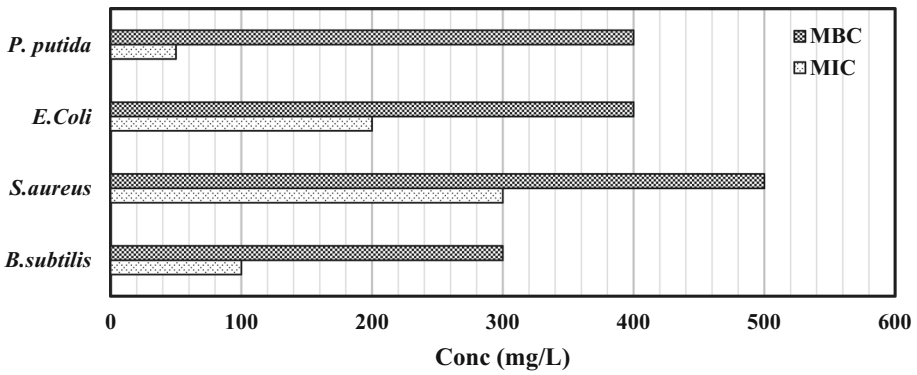

Fig. 7 Minimum Inhibitory Concentration (MIC) and Minimum Bactericidal Concentration (MBC) of test bacteria

Table 2 Average values of Zone of Inhibition (in mm) for Ag^0NP@GO nanocomposites of various concentrations against selected bacterial species

Conc (mg/L)	*B. subtilis*	*S. aureus*	*E. coli*	*P. putida*
0	–	–	–	–
25	–	–	–	–
50	–	–	–	12
100	18	–	–	12
200	19	11	11	14
300	20	14	11	16
400	21	14	18	18
500	21	18	21	21

of intercalated H_2O molecules trapped between hydrophilic graphene oxide sheets and the attachment of different oxide groups between the carbon layers is indicated by the rise in interlayer distance (d-spacing) when graphite oxidizes. From XRD pattern of the Ag^0NP@GO nanocomposite apart from the diffraction peak of GO concerted at 2θ of 10.7°, the peaks at 2θ = 38.19°, 44.38°, 64.53°,77.40° and 81.61° can be respectively indexed to the (111), (200), (220), (311) and (222) diffractions of metallic Ag nanoparticles, suggesting the successful formation of metallic Ag^0NP's on the surface of GO nanosheets. In-case of XRD difractogram of Ag^0NP@GO, intensity of GO peak position is little suppressed due to the surface decoration of GO nanosheet with Ag^0NPs [28]. According to Shrerrer's formula average particle size of the nanocomposite was observed to be 51 nm.

Figure 3 shows the Fourier transform infrared (FTIR) spectra of GO and Ag^0NP@GO. The C=C bonding of the aromatic rings of the GO carbon skeleton structure is represented by the existence of an absorption band at around 1591 cm^{-1}. The presence of other oxygenated functional groups can also be detected, including O–H stretching vibration at approximately 3424 cm^{-1} and O–H bending vibration at 1381 cm^{-1}, C=O stretching of carboxylic acid and or carbonyl moiety functional group at approximately 1729 cm^{-1}, C–O stretching with phenolic hydroxyl group C–OH bending observed at approximately 1209 cm^{-1}, and C–O at approximately 1051 cm^{-1} [71]. Similar observation were reported by Haldorai et al. [26] indicating successful formation of Ag^0NP@GO nanocomposite. However, the total removal of water could not be achieved as GO absorbs moisture from the air due to its hydrophilic groups (oxy, hydroxyl and epoxy) on GO nanosheet which was also detected in FTIR spectrum.

Scanning Electron Microscopy (SEM) micrographs were used to investigate the status of GO based silver nanocomposites after drying their dispersions. The top surface of the SEM images of the Ag^0NPs@GO nanocomposites revealed a thick surface, while many Ag^0NPs, white shiny dots (marked with a yellow arrow in Fig. 4), and were randomly distributed on the GO surface. They were in aggregates with uneven forms and a wide size distribution. HR-TEM analysis further revealed the deposition of Ag^0NP on the upper and lower layers of the crumpled silk waves like GO sheets (Fig. 5). The black-and-white contrast of the particles distinguishes between the depositions of Ag^0NP on translucent GO sheets.

Gao et.al [24] reported wrinkled Curtain like appearance of GO nanosheet proves a nano form of 2D carbon material. Further the purity of the synthesized Ag^0NPs was investigated by EDX spectral measurements (Table 1). The EDX spectra (Fig. 6) showed the presence of elemental composition of C (30.36%) and O (36.57%) atoms. The surface and in-situ anchoring of Ag^0NPs in GO nanosheet can be proved with very strong intensity of EDX spectra for Ag (33.06%). Thus, the aqueous extract of leaves of *Lantana camara* is found to be a powerful eco-friendly reducing agent for reducing metal salts into their nanostructures. Singh et.al [59] stated that nanoparticles synthesized from plant sources were found to be much more stable than those formed by microbes and fungus.

3.3 Inhibition of Bacterial Species using Synthesized Nanocomposite

A zone of inhibition (ZOI) test is a qualitative method to measure antimicrobial activity to inhibit microbial growth. It is an area of media where microorganism are unable to grow, due to presence of a nanocomposite that impedes their growth. Greater efficacy yields larger microbe-free zones surrounding nanocomposite containing well after overnight growth on solid media. *Staphylococcus aureus*, bacteria colonize the skin, gastrointestinal tract, and the blood stream infections are associated with significant mortality [62]. Pathogenic *E. coli* strains cause intestinal and extra-intestinal virulence by secreting the adhesins, toxins, iron acquisition factors, lipopolysaccharides that affect a wide range of cellular processes [36]. *Bacillus* and *Pseudomonas putida* are common in soil and water, but they have also been identified as opportunistic human pathogens that can cause nosocomial infections. [19]. Hence, inhibiting these bacteria is of great importance. From the antibacterial assay, it was observed that Ag^0NP@GO showed effective inhibitory action against all the test bacteria (Table 2). With the increase in the concentration of the nanocomposite inhibitory activity was also increased. Concentrations ranging from 25 to 500 mg/L were tested against selected bacterial species. *Pseudomonas putida* was most sensitive with zone of inhibition of 12 mm at 50 mg/L. At concentration of 100 mg/L only *B. subtilis* and *P. putida* were inhibited (ZOI–18 and 12 mm, respectively). To inhibit all four organism, minimum of 200 mg/L concentration of nanocomposite was required. *S. aureus* (ZOI–18 mm) resisted more at concentration of 500 mg/L as compared to other organisms (ZOI–21 mm). The cell wall and cell shape of Gram-positive bacteria, such as *S. aureus*, have many layers of peptidoglycan with 30–100 nm thickness, teichoic acid, and phosphated sugar [58] which make them resist to many antimicrobial. The results of Minimum Inhibitory Concentration and Minimum Bactericidal Concentration are in line with that of results of inhibition test. The MIC values for the Ag^0NP@GO nanocomposite were found to be 100 mg/L for *B. subtilis* and 300 mg/L for *S.aureus* (Fig. 7). Similar results i.e. no zone of inhibition for *S.aureus* at 100 mg/L and inhibition for *E.coli* were obtained by Chook et.al [12] where they used microwave-assisted technique for synthesis of similar nanocomposite. The MBC reported by Moraes et.al [50] against *S.aureus* and *E.coli* was 30 mg/L; however the synthesis of nanocomposite was through chemical reduction using sodium citrate. The gram-negative bacteria were more susceptible to the inhibitory action. This could be due to the presence of thin peptidoglycan layer present in the cell wall of gram-negative organism as compared to gram positive bacteria [4]. Overall, the antibacterial action of the Ag^0NP@GO nanocomposite can be explained as "Trap and Kill" mechanism. Where, GO nanosheet with 2D structure and surface functional groups and charges helps to bind the bacterial cells like a trapping agent and Ag^0NPs embedded in GO sheet makes the bacterial cell non-viable. Silver nanoparticles interact with bacterial membrane thereby altering the permeability and changing the cell structure leading to cell death [45]. According to Kurantowicz et al. [41], bacteria can cling to the GO surface, resulting in the highest

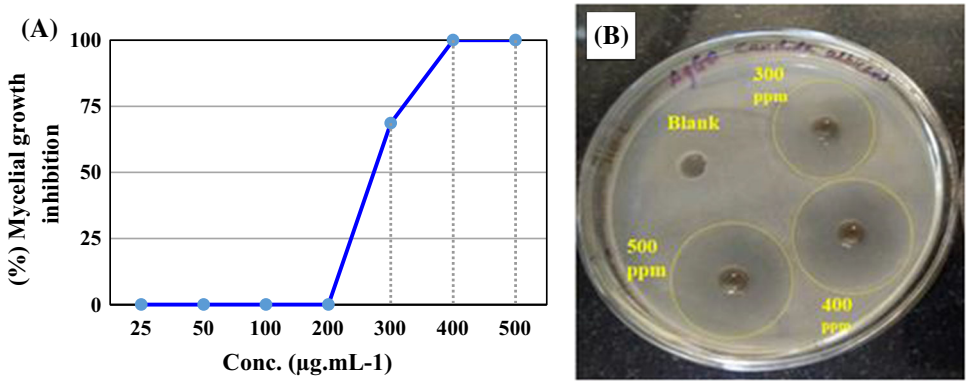

Fig. 8 **A** Percent (%) Mycelial growth inhibition of *Aspergillus niger* **B** Zone of Inhibition of *C. albicans*

Table 3 Antifungal Assay of *Aspergillus niger* and *Candida albicans*

	Diameter of Mycelial Growth (mm)	Zone of Inhibition in mm
Conc. (mg/L)	*Aspergillus niger*	*Candida albicans*
0	51	0
50	51	26
100	51	28
200	51	31
300	16	31
400	0	31
500	0	31

antibacterial activity. GO is characterized by a high degree of oxygenated functional groups: carbonyl, carboxylate, and hydroxyl which must be attracting bacteria since these groups are present on nutrients (amino acids, fatty acids).

3.4 Antifungal Activity of Synthesized Nanocomposite

Candida albicans is the most prevalent fungal pathogen in humans, causing infections ranging from mucosal to systemic. Biofilm production on the host or abiotic surfaces, such as indwelling medical devices, is linked to the majority of *C. albicans* infections, which are associated with high morbidity and death. Significantly, *C. albicans* biofilms are naturally resistant to antimicrobial therapy, hence its sensitivity to existing treatment drugs remains low [63]. The most common storage fungus, *Aspergillus niger,* is seen to constitute a severe threat to the food and herbal medicines industries. When living organisms, including humans, are exposed to *A. niger* and mycotoxins (ochratoxin A and fuminisins), usually are affected by immunotoxicity, carcinogenicity and hepatotoxicity [56]. Hence its inhibition is of utmost importance. The concentrations of Ag^0NP@GO nanocomposite, which totally inhibited the mycelial growths of *Aspergillus niger* was found to be 400 mg/L, whereas 300 mg/L had mild antifungal effect. Similar nanocomposite was used by Chen et.al [9] against *Fusarium graminearum* fungus. The agar well diffusion test performed on *Candida albicans* showed effective antifungal effect with increase in concentration. Very low concentration i.e. 50 mg/L could greatly inhibit *C.albicans* giving 26 mm zone of inhibition (Fig. 8 & Table 3). The zone of inhibition reported by Cui et.al [14] using same nanocomposite against *C.albicans* was 21 mm at 50 mg/L. Whereas, when silver nanoparticle in combination with other polymeric material like polyaniline and polystyrene showed mild antifungal activity against *C.albicans* compared to present work [69]. The ability of the Ag^0NP@GO nanosheets to suppress fungi is most likely due to direct contact with the fungi's cell walls. The reactive oxygen-containing functionalities of GO nanosheets might chemically react with the organic functional groups of chitin and other polysaccharides on the cell walls of fungi [30]. Ag^0NPs are well established for their antifungal properties, hence combination of GO with Ag^0 NPs acted synergistically against these pathogenic fungi.

The antimicrobial results obtained in this investigation were compared to those obtained in previous studies that used various types of nanoparticles or nanomaterials, synthesized using various processes, and tested against the bacteria used in this study. The Ag^0NP@GO preparation is simple and feasible, which is one of the major advantages of the synthesis process used in this research. We propose a cost-effective and

Table 4 Comparison of antimicrobial activity with the studies reported in the literature

Nanomaterial / Nanoparticle	Synthesis method	concentration used for ZOI	Microorganisms used for study Zone of Inhibition (ZOI in mm)						Reference
			B. subtilis	*S.aureus*	*E. coli*	*P. aeruginosa*	*A. niger*	*C. albicans*	
AgNPs	Cyanobacteria *Nostoc linckia* dried biomass as biological reducing agent	$AgNO_3$ 0.25 mM	0	0	0	0	0	0	Vanlalveni et al. [64]
		0.5 mM	8	9	8.3	14	10	0	
		1.0 mM	15	17	16	19	20	9	
Chitosan Coated Fe_3O_4 NPs	Fe_3O_4 NPs synthesized by co-precipitation method followed by coating of chitosan on Fe_3O_4 NPs	30 μg mL^{-1}	18		16	NA	15	16	Nehra et al. [52]
Copper NPs	Reduction of copper acetate with ethylene glycol and Tween 80 by refluxing around 200^0C for 3 Hrs	Not mentioned	NA	21	26	5	16	23	Ramyadevi et al. [55]
Green synthesized Cu NPs	*P. silesiensis* strain A3 protein coated CuNPs with size of 30.2 nm & negative charge of − 31 mv	1000 μg mL^{-1}	45	50	40	18	NA	40	Galal et al. [22]
Biogenic Synthesis of MgO-NPs	Biogenic agent as *Aspergillus terreus* S1	200 μg mL^{-1}	13	11	11	14	NA	12	Ebrahim et al. [17]
Mn_3O_4 nanoparticles	Precipitation method followed by calcination at 600 ^{0}C for 12 Hrs	30 μg mL^{-1}	18	19	10	12	–	18	Shaik et al. [57]

Table 4 (continued)

Nanomaterial / Nanoparticle	Synthesis method	concentration used for ZOI	Microorganisms used for study Zone of Inhibition (ZOI in mm)						Reference
			B. subtilis	*S.aureus*	*E. coli*	*P. aeruginosa*	*A. niger*	*C. albicans*	
Ag-MWCNTs	Wet-impregnation technique assisted with ultrasonication and calcination at 450 ^{0}C for 4 h under an inert atmosphere (N2 gas, 40 mL/min, 4 ^{0}C/min)	50 µL of 3% Ag-MWCNTs	16	15	14	-	13	13	Hamouda et al. [27]
		50 µL of 6% Ag-MWCNTs	18	17	17	17	17	16	
ZnO-NPs	Plant extract were heated with $ZnNO_3$ at 60 ^{0}C, calcined at 400 ^{0}C for 2 h to get ZnO	*Beta vulgaris* (BE1)	NA	0	10	NA	9	0	Pillai et al. [54]
		Cinnamomum tamala (VA1)	NA	8	8	NA	0	8	
		Cinnamomum verum (PA1)	NA	8	8	NA	0	0	
		Brassica oleracea (BR1)	NA	8	10	NA	8	8	
Ag^0NP@GO	Ag^0NP@GO synthesized using Lantana Camara extract	500 µg mL^{-1} Ag^0NP@GO	21	18	21	*P. putida* 21	Complete inhibition	31	This study

NA Not applicable

rapid synthesis method using the plant extract as compared to Shaik et al. [57], Hamouda et al. [27]. Furthermore, when compared to the data reported in Table 4, the antibacterial potential as ZOI was much higher. Except in the study by Galal et al. [22], when the dosage of protein coated CuNPs was 1000 μg/mL, which was twice as much as concentration used in current research work.

4 Conclusion

Ag^0NP@GO nanocomposites was successfully synthesized in situ with simple, inexpensive, environment friendly and non-toxic reaction set-up. Our method has the advantage that the GO surface acts as a suitable platform for deposition of Ag^0NPs to form composites for bio-related applications, using *Lantana camara* aqueous leaf extract as a green reductant for Ag^+ ions. This provides an alternative route of synthesis to minimize the usage of energy, corrosive and hazardous chemicals. Ag^0NP with an average size of 76 nm were impregnated onto GO sheets. Ag^0NP@GO nanocomposites showed effective antibacterial activity and antifungal activity. The advantage of this surface functionalized nanocomposite with low Ag content is that it reduces the concern and risk of excessive silver use, making it a potential material for disinfection applications and an effective solution for public health. In conclusion, Ag^0NP@GO nanocomposites has proven to be a promising nanocomposite for controlling harmful biological contaminants.

Acknowledgements One of the authors, Mr. Abhaysinh R Salunkhe is grateful to CSIR-HRDG for awarding Senior Research Fellowship (CSIR SRF). We also would like to thank the technical and administrative support from NEERI Mumbai Zonal Laboratory—Research and Innovation Centre, SAIF-IIT Bombay and CSIR-NEERI, Nagpur.

Declarations

Conflict of Interest The authors declare that they have no conflict of interests regarding the publication of this paper.

References

1. Abdelghany, T.M.; Al-Rajhi, A.M.H.; Al Abboud, M.A.; Alawlaqi, M.M.; Ganash Magdah, A.; Helmy, E.A.M.; Mabrouk, A.S.: Recent advances in green synthesis of silver nanoparticles and their applications: about future directions. Rev. BioNanoSci (2017). https://doi.org/10.1007/s12668-017-0413-3
2. Aboulthana, W.M.; Ibrahim, N.S.; Osman, N.M.; Seif, M.M.; Hassan, A.K.; Youssef, A.M.; El-Feky, A.M.; Madboli, A.A.: Evaluation of the biological efficiency of silver nanoparticles biosynthesized using Croton tiglium L. seeds extract against Azoxymethane induced colon cancer in rats. Asian Pacific J. Cancer. Prevent. (2020). https://doi.org/10.31557/APJCP.2020.21.5.1369
3. Allen, M.J.; Tung, V.C.; Kaner, R.B.: Honeycomb Carbon: A Review of Graphene. Chem. Rev. (2009). https://doi.org/10.1021/cr900070d
4. An, S.S.A.; Nanda, S.S.; Yi, D.K.: Oxidative stress and antibacterial properties of a graphene oxide-cystamine nanohybrid. Int. J. Nanomed. (2015). https://doi.org/10.2147/ijn.s75768
5. Azrul, L.M.; Nurulaini, R.; Adzemi, M.A.; Marina, H.; Effendy, A.W.M.: Tannins quantification in terminalia catappa leaves extract and antihelmenthic potential evaluation. J. Natural Products **7**, 98–103 (2014)
6. Brown, T.; Smith, D.: The effects of silver nitrate on the growth and ultrastructure of the yeast *Cryptococcus albidus*. Microbios Lett. **3**, 155–162 (1976)
7. Cai, X.; Lin, M.; Tan, S.; Mai, W.; Zhang, Y.; Liang, Z.; Lin, Z.; Zhang, X.: The use of polyethyleneimine-modified reduced graphene oxide as a substrate for silver nanoparticles to produce a material with lower cytotoxicity and long-term antibacterial activity. Carbon (2012). https://doi.org/10.1016/j.carbon.2012.02.002
8. Chen, J.W.; Lee, G.W.M.; Chen, K.J.; Yang, S.H.: Control of bioaerosols in indoor environment by filter coated with nanosilicate platelet supported silver nanohybrid (AgNPs/NSP). Aerosol. Air Quality Res. (2016). https://doi.org/10.4209/aaqr.2016.06.0224
9. Chen, J.; Sun, L.; Cheng, Y.; Lu, Z.; Shao, K.; Li, T.; Hu, C.; Han, H.: Graphene oxide-silver nanocomposite: novel agricultural antifungal agent against *Fusarium graminearum* for crop disease prevention. ACS Appl. Mater. Interfaces. (2016). https://doi.org/10.1021/acsami.6b05730
10. Cheng, H.H.; Hsieh, C.C.; Tsai, C.H.: Antibacterial and regenerated characteristics of Ag-zeolite for removing bioaerosols in indoor environment. Aerosol. Air Quality Res. (2012). https://doi.org/10.4209/aaqr.2011.08.0134
11. Chettri, P.; Vendamani, V.; Tripathi, A.; Singh, M.K.; Pathak, A.P.; Tiwari, A.: Green synthesis of silver nanoparticle-reduced graphene oxide using Psidium guajava and its application in SERS for the detection of methylene blue. Appl. Surf. Sci. (2017). https://doi.org/10.1016/j.apsusc.2017.02.073
12. Chook, S.; Chia, C.; Zakaria, S.; Ayob, M.; Chee, K.; Huang, N.; Neoh, H.; Lim, H.; Jamal, R.; Rahman, R.: Antibacterial performance of Ag nanoparticles and AgGO nanocomposites prepared via rapid microwave-assisted synthesis method. Nanoscale. Res. Lett. (2012). https://doi.org/10.1186/1556-276x-7-541
13. Chopra, I.: The increasing use of silver-based products as antimicrobial agents: a useful development or a cause for concern? J. Antimicrob. Chemother. **60**(2), 447–448 (2007)
14. Cui, J.; Yang, Y.; Zheng, M.; Liu, Y.; Xiao, Y.; Lei, B.; Chen, W.: Facile fabrication of graphene oxide loaded with silver nanoparticles as antifungal materials. Mater. Res. Express (2014). https://doi.org/10.1088/2053-1591/1/4/045007
15. Das, M.R.; Sarma, R.K.; Saikia, R.; Kale, V.S.; Shelke, M.V.; Sengupta, P.: Synthesis of silver nanoparticles in an aqueous suspension of graphene oxide sheets and its antimicrobial activity. Colloids Surf., B (2011). https://doi.org/10.1016/j.colsurfb.2010.10.033
16. Deena, M.J.; Thoppil, J.E.: Antimicrobial activity of the essential oil of Lantana camara. Fitoterapia **71**(4), 453–455 (2000)
17. Ebrahim, S.; Eid, A.M.; Hassan, S.E.-D.; Salem, S.S.; Radwan, A.A.; Halawa, M.; Saleh, F.M.; Saad, H.A.; Saied, E.M.; Fouda, A.: The catalytic activity of biosynthesized magnesium oxide nanoparticles (MgO-NPs) for inhibiting the growth of pathogenic microbes, tanning effluent treatment, and chromium ion removal. Catalysts. **11**(7), 821 (2021). https://doi.org/10.3390/catal11070821
18. FAO/IAEA, (2000) Laboratory manual, quantification of tannins in tree foliage, "Co-ordinated research project on 'use of nuclear and related techniques to develop simple tannin assays for predicting and improving the safety and efficiency of feeding ruminants on tanniniferous tree Foliage', Working Document, IAEA, VIENNA

19. Fernandez, M.; Porcel, M.; de la Torre, J.; Molina-Henares, M.A.; Daddaoua, A.; Llamas, M.A.; Roca, A.; Carriel, V.; Garzón, I.; Ramos, J.L.; Alaminos, M.; Duque, E.: Analysis of the pathogenic potential of nosocomial *Pseudomonas putida* strains. Front. Microbiol. (2015). https://doi.org/10.3389/fmicb.2015.00871
20. Francis, S.; Joseph, S.; Koshy, P.; Mathew, B.: Microwave assisted green synthesis of silver nanoparticles using leaf extract of *Elephantopus scaber* and its environmental and biological applications. Artif. Cells. Nanomed. Biotechnol. **46**, 795–804 (2017). https://doi.org/10.1080/21691401.2017.1345921
21. de Freitas Rosa, P.; Aguiar, M.L.; Bernardo, A.: Modification of cotton fabrics with silver nanoparticles for use in conditioner air to minimize the Bioaerosol concentration in indoor environments. Water, Air, Soil Pollution. (2017). https://doi.org/10.1007/s11270-017-3429-y
22. Galal, G. F.; Abd-Elhalim, B. T.; Abou-Taleb, K. A.; Haroun, A. A.; Gamal, R. F.: Toxicity assessment of green synthesized Cu nanoparticles by cell-free extract of Pseudomonas silesiensis as antitumor cancer and antimicrobial. Annal. Agricultur Sci. **66**(1), 8–15 (2021). https://doi.org/10.1016/j.aoas.2021.01.006
23. Ganjewala, D.; Sam, S.; Khan, K.H.: Biochemical compositions and antibacterial activities of Lantana camara plants with yellow, lavender, red and white flowers. EurAsian J. BioSci. **3**(1), 69–77 (2009)
24. Gao, R.; Hu, N.; Yang, Z.; Zhu, Q.; Chai, J.; Su, Y.; Zhang, L.; Zhang, Y.: Paper-like graphene-Ag composite films with enhanced mechanical and electrical properties. Nanoscale. Res. Lett. (2013). https://doi.org/10.1186/1556-276x-8-32
25. Ghisalberti, E.L.: Lantana camara L. (verbenaceae). Fitoterapia **71**(5), 467–486 (2000)
26. Haldorai, Y.; Kim, B.K.; Jo, Y.L.; Shim, J.J.: Ag@graphene oxide nanocomposite as an efficient visible-light plasmonic photocatalyst for the degradation of organic pollutants: A facile green synthetic approach. Mater. Chem. Phys. (2014). https://doi.org/10.1016/j.matchemphys.2013.11.065
27. Hamouda, H.I.; Abdel-Ghafar, H.M.; Mahmoud, M.H.H.: Multi-walled carbon nanotubes decorated with silver nanoparticles for antimicrobial applications. J. Environ. Chem. Eng. (2021). https://doi.org/10.1016/j.jece.2021.105034
28. He, Y.; Cui, H.: Synthesis of highly chemiluminescent graphene oxide/silver nanoparticle nano-composites and their analytical applications. J. Mater. Chem. (2012). https://doi.org/10.1039/c2jm16028e
29. Huang, N.M.: Simple room-temperature preparation of high-yield large-area graphene oxide. Int. J. Nanomed. (2011). https://doi.org/10.2147/ijn.s26812
30. Hudler, G.W.: Magical mushrooms mischievous molds, p. 7–7. Princeton University, Princeton, NJ (1998)
31. Irshad, M.; Zafaryab, M.; Singh, M.; Rizvi, M.M.A.: Comparative analysis of the antioxidant activity of cassia fistula extracts. Int. J. Med. Chem. (2012). https://doi.org/10.1155/2012/157125
32. Jain, D.; Daima, H.; Kachhwala, S.; Kothari, S.: Synthesis of plant mediated silver nanoparticles using papaya fruit extract and evaluation of their anti-microbial activities. Dig. J. Nanomater. Biostruct. **4**, 557–563 (2009)
33. Jain, R.; Singh, M.; Dezman, D.J.: Qualitative and quantitative characterization of phenolic compounds from lantana (Lantana camara) leaves. Weed Sci. (1989). https://doi.org/10.1017/s0043174500071964
34. Jiang, Y.; Liu, D.; Cho, M.; Lee, S.S.; Zhang, F.; Biswas, P.; Fortner, J.D.: In situ photocatalytic synthesis of Ag nanoparticles (nAg) by crumpled graphene oxide composite membranes for filtration and disinfection applications. Environ. Sci. Technol. (2016). https://doi.org/10.1021/acs.est.5b04584
35. Jung, J.H.; Hwang, G.B.; Lee, J.E.; Bae, G.N.: Preparation of airborne Ag/CNT hybrid nanoparticles using an aerosol process and their application to antimicrobial air filtration. Langmuir (2011). https://doi.org/10.1021/la201851r
36. Kaper, J.; Nataro, J.; Mobley, H.: Pathogenic *Escherichia coli*. Nat. Rev. Microbiol. (2004). https://doi.org/10.1038/nrmicro818
37. Kesharwani, J.; Yoon, K.Y.; Hwang, J.; Rai, M.: Phytofabrication of silver nanoparticles by leaf extract of Datura metel: hypothetical mechanism involved in synthesis. J. Bionanosci. **3**(1), 39–44 (2009)
38. Ko, Y.S.; Joe, Y.H.; Seo, M.; Lim, K.; Hwang, J.; Woo, K.: Prompt and synergistic antibacterial activity of silver nanoparticle-decorated silica hybrid particles on air filtration. J. Mater. Chem. B (2014). https://doi.org/10.1039/c4tb01068j
39. Kong, H.; Jang, J.: Antibacterial properties of Novel Poly (methyl methacrylate) nanofiber containing silver nanoparticles. Langmuir (2008). https://doi.org/10.1021/la703085e
40. Kumar, S.; Sandhir, R.; Ojha, S.: Evaluation of antioxidant activity and total phenol in different varieties of *Lantana camara* leaves. BMC. Res. Notes (2014). https://doi.org/10.1186/1756-0500-7-560
41. Kurantowicz, N.; Sawosz, E.; Jaworski, S.; Kutwin, M.; Strojny, B.; Wierzbicki, M.; Szeliga, J.; Hotowy, A.; Lipińska, L.; Koziński, R.; Jagiełło, J.; Chwalibog, A.: Interaction of graphene family materials with *Listeria monocytogenes* and *Salmonella enterica*. Nanoscale. Res. Lett. (2015). https://doi.org/10.1186/s11671-015-0749-y
42. Li, J.; Kuang, D.; Feng, Y.; Zhang, F.; Xu, Z.; Liu, M.; Wang, D.: Green synthesis of silver nanoparticles-graphene oxide nanocomposite and its application in electrochemical sensing of tryptophan. Biosens. Bioelectron. (2013). https://doi.org/10.1016/j.bios.2012.10.029
43. Liu, Y.; Tian, C.; Yan, B.; Lu, Q.; Xie, Y.; Chen, J.; Gupta, R.; Xu, Z.; Kuznicki, S.M.; Liu, Q.; Zeng, H.: Nanocomposites of graphene oxide, Ag nanoparticles, and magnetic ferrite nanoparticles for elemental mercury (Hg^0) removal. RSC Adv. (2015). https://doi.org/10.1039/C4RA16016A
44. Liu, H.; Zhong, L.; Yun, K.; Samal, M.: Synthesis, characterization, and antibacterial properties of silver nanoparticles-graphene and graphene oxide composites. Biotechnol. Bioprocess Eng. (2016). https://doi.org/10.1007/s12257-015-0733-5
45. Lok, C.N.; Ho, C.M.; Chen, R.; He, Q.Y.; Yu, W.Y.; Sun, H.; Tam, P.K.H.; Chiu, J.F.; Che, C.M.: Proteomic analysis of the mode of antibacterial action of silver nanoparticles. J. Proteome Res. **5**(4), 916–924 (2006). https://doi.org/10.1021/pr0504079
46. Magaldi, S.; Mata-Essayag, S.; Hartung, C.: Well diffusion for antifungal susceptibility testing. Int. J. Infect. Dis. **8**, 39–45 (2004)
47. Martínez-Orozco, R.D.; Rosu, H.C.; Lee, S.W.; Rodríguez-González, V.: Understanding the adsorptive and photoactivity properties of Ag-graphene oxide nanocomposites. J Hazardous Mater (2013). https://doi.org/10.1016/j.jhazmat.2013.07.056
48. McFarland, J.: The nephelometer: an instrument for estimating the number of bacteria in suspensions used for calculating the opsonic index and for vaccines. JAMA J. Am. Med. Assoc. **49**, 1176–8 (1907). https://doi.org/10.1001/jama.1907.25320140022001f
49. Mock, J.; Barbic, M.; Smith, R.; Schultz, A.; Schultz, S.: Shape effects in Plasmon resonance of individual colloidal silver nanoparticles. J. Chem. Phys. **116**, 6755–6759 (2002)
50. Moraes, M.D.; Araujo Lima, B.; Fonseca de Faria, A.; Brocchi, M.; Luiz Alves, O.: Graphene oxide-silver nanocomposite as a promising biocidal agent against methicillin-resistant Staphylococcus aureus. Int. J. Nanomed. (2015). https://doi.org/10.2147/ijn.s90660
51. Nagah, S.; Saada, G.; Abdel-Maksoud, M.S.; El-Aziz, Abd; Youssef, A.M.: Green synthesis of silver nanoparticles, characterization, and use for sustainable preservation of historical parchment against microbial biodegradation. Biocatal. Agricultur. Biotechnol. **32**, 101948 (2021)

52. Nehra, P.; Chauhan, R.P.; Garg, N.; Verma, K.: Antibacterial and antifungal activity of chitosan coated iron oxide nanoparticles. Br. J. Biomed. Sci. (2018). https://doi.org/10.1080/09674845.2017.1347362
53. Pasricha, R.; Gupta, S.; Joshi, A.G.; Bahadur, N.; Haranath, D.; Sood, K.N.; Singh, S.; Singh, S.: Directed nanoparticle reduction on graphene. Mater. Today (2012). https://doi.org/10.1016/s1369-7021(12)70047-0
54. Pillai, A.M.; Sivasankarapillai, V.S.; Rahdar, A.; Joseph, J.; Sadeghfar, F.; Rajesh, K.; Kyzas, G.Z.: Green synthesis and characterization of zinc oxide nanoparticles with antibacterial and antifungal activity. J. Mole. Struct. **1211**, 128107 (2020). https://doi.org/10.1016/j.molstruc.2020.128107
55. Ramyadevi, J.; Jeyasubramanian, K.; Marikani, A.; Rajakumar, G.; Rahuman, A.A.: Synthesis and antimicrobial activity of copper nanoparticles. Mater. Lett. (2012). https://doi.org/10.1016/j.matlet.2011.12.055
56. Schuster, E.; Dunn-Coleman, N.; Frisvad, J.C.; Dijck, P.: On the safety of *Aspergillus niger* – a review. Appl. Microbiol. Biotechnol. (2002). https://doi.org/10.1007/s00253-002-1032-6
57. Shaik, M.R.; Syed, R.; Adil, S.F.; Kuniyil, M.; Khan, M.; Alqahtani, M.S.; Shaik, J.P.; Siddiqui, M.R.H.; Al-Warthan, A.; Sharaf, M.A.; Abdelgawad, A.: Mn3O4 nanoparticles: Synthesis, characterization and their antimicrobial and anticancer activity against A549 and MCF-7 cell lines. Saudi J. Biol. Sci. (2021). https://doi.org/10.1016/j.sjbs.2020.11.087
58. Silhavy, J.; Kahne, D.; Walker, S.: The bacterial cell envelope. Cold Spring Harbor Pers. Boil. **2**(5), a000414 (2010)
59. Singh, P.; Kim, Y.J.; Zhang, D.; Yang, D.C.: Biological synthesis of nanoparticles from plants and microorganisms. Trends. Biotechnol. (2016). https://doi.org/10.1016/j.tibtech.2016.02.006
60. Sinitskii, A.; Sun, Z.; Slesarev, A.; Alemany, L.B.; Lu, W.; Tour, J.M.: Improved synthesis of graphene oxide. ACS. Nano. **4**(8), 4806–4814 (2010)
61. Soroush, A.; Ma, W.; Silvino, Y.; Saifur Rahaman, M.D.: Surface modification of thin film composite forward osmosis membrane by silver-decorated graphene-oxide nanosheets. Environ. Sci. Nano **2**, 395 (2015). https://doi.org/10.1039/C5EN00086F
62. Thomer, L.; Olaf, S.; Missiakas, D.: Pathogenesis of *Staphylococcus aureus* Bloodstream Infections. Annu. Rev. Pathol. **11**(1), 343–364 (2016)
63. Tsui, C.; Eric, F.; Kong, J.R.: Pathogenesis of *Candida albicans* biofilm. Pathogens. Disease (2016). https://doi.org/10.1093/femspd/ftw018
64. Vanlalveni, C.; Rajkumari, K.; Biswas, A., et al.: Green synthesis of silver nanoparticles using nostoc linckia and its antimicrobial activity: a novel biological approach. BioNanoSci. (2018). https://doi.org/10.1007/s12668-018-0520-9
65. Yakabe, Y.; Sano, T.; Ushio, H.; Yasunaga, T.: Kinetic studies of the interaction between silver ion and deoxyribonucleic acid. Chem. Lett. (1980). https://doi.org/10.1246/cl.1980.373
66. Yoon, K.Y.; Byeon, J.H.; Park, C.W.; Hwang, J.: Antimicrobial effect of silver particles on bacterial contamination of activated carbon fibers. Environ. Sci. Technol. (2008). https://doi.org/10.1021/es0720199
67. Youngmin, S.; Jangsun, H.; Jieun, K.; Yoon, J.; Mintai, P.H.; Jonghoon, C.: Antibacterial activity and cytotoxicity of multiwalled carbon nanotubes decorated with silver nanoparticles. Int. J. Nanomed. **9**, 4621–4629 (2014)
68. Youssef, A.M.; Hasanin, M.S.; El-Aziz, M.E.A.: Conducting chitosan/hydroxylethyl cellulose/polyaniline bionanocomposites hydrogel based on graphene oxide doped with Ag-NPs. Int. J. Biol. Macromol. (2021). https://doi.org/10.1016/j.ijbiomac.2020.11.097
69. Youssef, A.M.; Mohamed, S.A.; Abdel-Aziz, M.S.; Abdel-Aziz, M.E.; Turky, G.; Kamel, S.: Biological studies and electrical conductivity of paper sheet based on PANI/PS/Ag-NPs nanocomposite. Carbohyd. Polym. (2016). https://doi.org/10.1016/j.carbpol.2016.03.085
70. Yuvaraj, H.; Kim, B.K.; Jo, Y.L.; Shim, J.J.: Ag@graphene oxide nanocomposite as an efficient visible-light plasmonic photocatalyst for the degradation of organic pollutants: A facile green synthetic approach. Mater. Chem. Phys. (2014). https://doi.org/10.1016/j.matchemphys.2013.11.065
71. Zhu, C.; Guo, S.; Fang, Y.; Dong, S.: Reducing sugar: new functional molecules for the green synthesis of graphene nanosheets. ACS. Nano. **4**, 2429–37 (2010). https://doi.org/10.1021/nn1002387